Experimental Eye Research 163 (2017) 72–77

Contents lists available at ScienceDirect

Experimental Eye Research

journal homepage: www.elsevier.com/locate/yexer

Review

# Morphological evaluation for diagnosis of dry eye related to meibomian gland dysfunction

Young-Sik Yoo [a, b], Kyung-Sun Na [c], Dae Yu Kim [d], Suk-Woo Yang [e], Choun-Ki Joo [b, e, *]

[a] Department of Convergence Medical Science, College of Medicine, The Catholic University of Korea, Seoul, South Korea
[b] Catholic Institute for Visual Science, College of Medicine, The Catholic University of Korea, Seoul, South Korea
[c] Department of Ophthalmology and Visual Science, College of Medicine, Yeouido St. Mary's Hospital, The Catholic University of Korea, Seoul, South Korea
[d] Electrical Engineering, College of Engineering, Inha University, Incheon, South Korea
[e] Department of Ophthalmology and Visual Science, College of Medicine, Seoul St. Mary's Hospital, The Catholic University of Korea, Seoul, South Korea

ARTICLE INFO

*Article history:*
Received 1 April 2017
Received in revised form
11 July 2017
Accepted in revised form 11 July 2017

*Keywords:*
Meibomian glands
Dry eye disease
Optical coherence tomography

ABSTRACT

The evaluation of morphological changes of the acini in the meibomian glands is important for the diagnosis and management of dry eye related to meibomian gland dysfunction. While several tools have been developed to detect meibomian gland structure, infrared imaging is generally used in clinical settings. Unlike the lipid component analysis of tear film in which quantitative analysis is possible, the meibomian glands are limited to qualitative analysis because of the low image quality of the diagnostic tools. This review describes diagnostic tools, especially in terms of morphological evaluation of the acini, which are visualized by the existence of lipid within them.



**Contents**

1. Development of diagnostic tools for meibomian gland dysfunction ..... 73
2. Infrared meibography ..... 73
3. OCT meibography ..... 74
4. Quantification of the acinar area in the meibomian glands ..... 74
5. Future of meibomian gland dysfunction diagnosis ..... 76
6. Funding ..... 76
Conflict of interest ..... 76
References ..... 76

## 1. Introduction[1]

The lipid component from the meibomian glands is essential for the maintenance of the tear film and related to ocular surface health and integrity (Arita et al., 2008; Knop et al., 2011; Nicolaides et al., 1981). The evaporation of the aqueous component in the tear film is affected by its lipid component (Nichols et al., 2011). Meibomian gland dysfunction (MGD) occurs from the change of the lipid quality in tear film or the secretory function of the lipid component caused by low delivery and high delivery states of meibomian gland secretion (Geerling et al., 2017; Nelson et al., 2011). Several studies have reported that MGD was

*Abbreviations:* IR, Infrared; MGD, Meibomian gland dysfunction; OCT, Optical coherence tomography; OCM, Optical coherence microscopy.

* Corresponding author. Department of Ophthalmology and Visual Science, College of Medicine, Seoul St. Mary's Hospital, The Catholic University of Korea, 222 Banpo-daero, Seocho-gu, Seoul 06591, South Korea.
*E-mail address:* ckjoo@catholic.ac.kr (C.-K. Joo).

[1] **Abbreviations:** 2D, two-dimensional; 3D, three-dimensional; IR, infrared; MGD, meibomian gland dysfunction; OCM, optical coherence microscopy; OCT, optical coherence tomography.

http://dx.doi.org/10.1016/j.exer.2017.07.005
0014-4835/

observed in a large portion of patients with dry eye and is currently noted as one of the main causes of dry eye (Bron and Tiffany, 2004; Geerling et al., 2017; Lemp et al., 2012; Qiao and Yan, 2013; Tong et al., 2010).

Despite the importance of MGD, diagnostic criteria for MGD have not been completely established to date. Moreover, several diagnostic tools have been introduced and then disappeared for evaluation of the lipid component in the tear film or acini. Diagnostic tools, especially with respect to morphological evaluation of the acini, are discussed in this brief review.

## 2. Development of diagnostic tools for meibomian gland dysfunction

Several diagnostic tools have been developed to diagnose MGD. Tear osmolarity, tear break-up time, oil imprinting, and lipid layer thickness aim to measure the lipid component in the tear film (Finis et al., 2013; Tomlinson et al., 2011). The functional aspects of MGD are evaluated by the effects of the appropriate lipid amount and quality on tear film stability. In contrast, imaging techniques including transillumination (Jester et al., 1982; Robin et al., 1985; Tapie, 1977; Yokoi et al., 2007), non-contact infrared (IR) light (Arita et al., 2008), confocal microscopy (Matsumoto et al., 2008; Messmer et al., 2005; Villani et al., 2011), and optical coherence tomography (OCT, Hwang et al., 2013); provide morphological evaluations of the meibomian glands (Fig. 1) (Pult and Nichols, 2012; Tomlinson et al., 2011).

Background information from a morphological evaluation of the meibomian glands such as the acini or ducts would support a diagnosis of MGD. Recently, newly proposed diagnostic and grading tools for MGD have included meibomian gland dropout as one of the parameters (Arita et al., 2016; Milner et al., 2017; Nichols et al., 2011; Tsubota et al., 2017). Articles have emphasized the importance of morphological evaluation as well as a grading system. Moreover, gland dropout was divided into whole gland dropout and partial gland dropout by Arita et al. (2016) in a new grading scale for MGD.

Transillumination was first introduced to visualize the detailed structure of the meibomian glands by Tapie (1977). A contact tool such as a plate or probe-type illuminator must be utilized for measurement, and complete contact between the eyelid and contact tool guarantees good image quality. IR transillumination imaging was introduced by Jester et al. (1982); they obtained meibomian gland images from rabbits. Arita et al. (2008) first introduced IR meibography as a non-contact method. Later, confocal microscopy and OCT techniques were introduced to visualize the detailed structure of the meibomian glands more precisely (Hwang et al., 2013; Matsumoto et al., 2008; Messmer et al., 2005; Villani et al., 2011). The features of each device were described in Table 1.

## 3. Infrared meibography

IR imaging has been the most widely used tool for detecting gland dropout in patients with MGD. IR imaging can be obtained by adding an IR-transmitting filter and IR-sensitive camera to detect IR light from a slit lamp in an outpatient clinic (Arita et al., 2008). In addition to the simplicity of IR imaging, one image is sufficient to cover the entire area of the meibomian glands located in the upper and lower eyelids. Arita et al. (2009a, 2009b, 2010, 2016) reported the efficacy of IR imaging as well as diagnostic criteria for evaluating MGD.

Because the commercial IR noncontact meibography systems use shorter wavelength IR (800–940 nm [Arita et al., 2014; Kent, 2013; Srinivasan et al., 2012]) than that of OCT (1300 nm), IR noncontact meibography is limited to penetrating the palpebral conjunctiva. Meibomian glands are located beyond the palpebral conjunctiva and the palpebral conjunctiva in patients with MGD had a tendency to be thickened compared with those of subjects without dry eye disease (Liang et al., 2015). As a result, there are some limitations to IR imaging. One is that IR meibography provides a frontal-plane two-dimensional (2D) image created by overlapping all images from a limited range of depths. Thus, the acquired images have no depth information about the meibomian glands. The other limitation is caused by a misunderstanding of the obtained images because of the different contrasts obtained according to the strength of the external light source (Fig. 2). In contrast to IR imaging, there is almost no change in image quality depending on the intensity of the light source in OCT imaging (Leitgeb et al., 2003). However, commercial devices such as the Keratograph® 5M (K5M; Wetzlar, Germany), Cobra® fundus camera (CSO and bon Optic VertriebsgmbH, Germany), and LipiView® (TearScience Inc., Morrisville, NC, USA) provide contrast enhancement for acquired images using software in the devices. Additionally, when grading gland dropout using a linear four-point integer scale, a high rate of disagreement was reported between two different IR images from two IR non-contact meibography modalities due to image quality differences (Ngo et al., 2014).

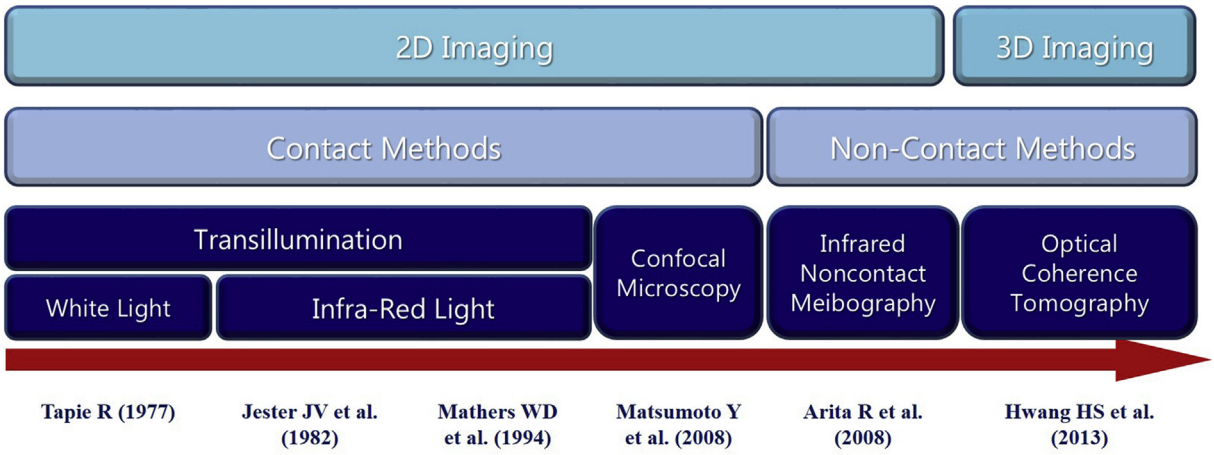


**Fig. 1.** Development of the imaging technique for visualizing meibomian gland morphology.

**Table 1**
Comparison of infrared non-contact meibography, confocal microscopy, and optical coherence meibography.

| | IR Non-contact Meibography | Confocal Microscopy | OCT Meibography[d] |
|---|---|---|---|
| Field-of-View | It is possible to include almost all the meibomian glands in the upper or lower eyelid in one image | 400 × 400 μm[a] | 4.3 × 4.3 mm |
| Advantages | Available in the clinical field<br>Fast IR image acquisition | Extensive examination of acini (acinar density and diameter, inflammation around acini, and secretion reflectivity)[b]<br>Imaging resident *Demodex* mites[c] | Provides depth information<br>Enhanced visibility (detailed conformations of acini and/or ducts) |
| Disadvantages | No depth information<br>Misunderstanding due to the intensity of the light source<br>Disagreement between different IR images due to image quality differences | Does not include all the meibomian glands in the upper or lower eyelid in one image (small field of view)<br>Requires a learning curve to obtain a quality image<br>Requires the use of topical anesthesia | Does not include all the meibomian glands in the upper or lower eyelid in one image<br>No commercially available device<br>Motion artifacts caused by pulsation or breathing occur for approximately 5 s during the examination<br>Requires a long time to render a 3D image |

3D = three-dimensional, IR = infrared, OCT = optical coherence tomography.
[a] Field-of-view for confocal microscopy was based on the studies by Ibrahim et al. (2010, 2012) and Matsumoto et al. (2008).
[b] Matsumoto et al. (2008); Messmer et al. (2005); Villani et al. (2011).
[c] Randon et al. (2015).
[d] Detailed values for OCT meibography are based on the study by Yoo et al. (2017).

## 4. OCT meibography

*In vivo* 3D images of the meibomian glands using OCT was first introduced by Hwang et al. (2013) and OCT imaging could provide depth information and enhanced visibility compared with IR images. Although IR images could confirm definitely abnormal structures of the meibomian glands including gland dropout, the images cannot confirm the anatomic details of the gland structures (Yoo et al., 2017). A high-speed swept-source laser system (50 KHz) used a 1300-nm OCT light source to penetrate the bottom layer of the meibomian glands. Comparison studies using light sources of different wavelengths demonstrated that a 700-nm light source had 4.3 times greater scattering and absorption coefficients in the epidermal skin than those of a 1300-nm light (Salomatina et al., 2006; Tuchin, 2007). These characteristics of longer-wavelength light improved the OCT imaging depth and enabled visualization of deeper regions of the meibomian glands. In IR imaging, however, high scattering around 700-nm lights could lead to blurriness in images acquired from the frontal layer of the meibomian glands (Yoo et al., 2017).

OCT images yielded detailed conformations of acini and/or ducts (in the case in which there is no stricture above the ducts, as shown in Fig. 3B) in the deep layer of the meibomian glands and dropout lesions, which could not be obtained via IR imaging (Fig. 3). The portion where there is no actual structure (Fig. 3C) appears as a dropout on both IR and OCT imaging. The portion where the structure actually exists cannot be seen as a dropout on IR imaging (Fig. 3B Left), but the structure can be seen on OCT imaging (Fig. 3B Right). OCT images included the acinar and ductal structures located in the deep layer while IR could not detect these structures because of its short penetration depth compared with OCT. Recently, some studies have reported that OCT images provided more detailed structures of deep-layer meibomian glands compared with IR imaging (Liang et al., 2015; Napoli et al., 2016; Yoo et al., 2017). However, OCT meibography has some limitations in the measurement area, which cannot cover the entire area of the meibomian glands in the eyelids, and data processing for rendering three-dimensional (3D) images requires a long duration. The other limitation is that the clinical ophthalmologist cannot use OCT meibography, unlike non-contact meibography.

## 5. Quantification of the acinar area in the meibomian glands

Our study provided anatomic details of meibomian gland dropout by using OCT meibography and IR imaging (Yoo et al., 2017). Although OCT imaging could be considered to determine actual losses of or changes in the meibomian glands, a quantitative analysis of acinar size is necessary to determine their actual function in the meibomian glands. Throughout the segmentation methods, the quantification of acini was performed using OCT meibography. Sharp-margin OCT images of the acini were not obtained because of a relatively small difference in the index of refraction between acini (meibocytes) and tarsus as well as their overlapping boundaries. Hence, we performed an *ex vivo* study using human upper eyelid specimens to obtain good-quality OCT of the acini.

Measuring the area of the acini at different depths from each OCT image would support the availability of a method for diagnosing MGD. Fig. 4 shows an example of measuring acinar areas at three different depths of the meibomian glands. Each acinar area was calculated in pixels to provide numerical values (Fig. 5). Quantification of the acini in the meibomian glands through

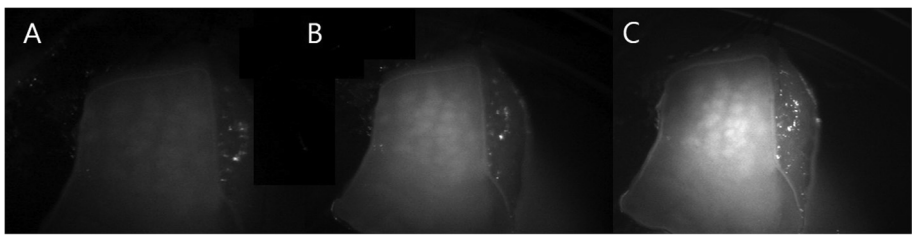


**Fig. 2.** Representative images showing different image qualities according to the intensity of the light source when measuring infrared (IR) images of the meibomian glands. A human upper eyelid specimen was used in this comparison and it was taken by non-contact IR meibography, which was composed of an IR-transmitting filter and an IR-sensitive camera introduced by Arita et al. (2008).

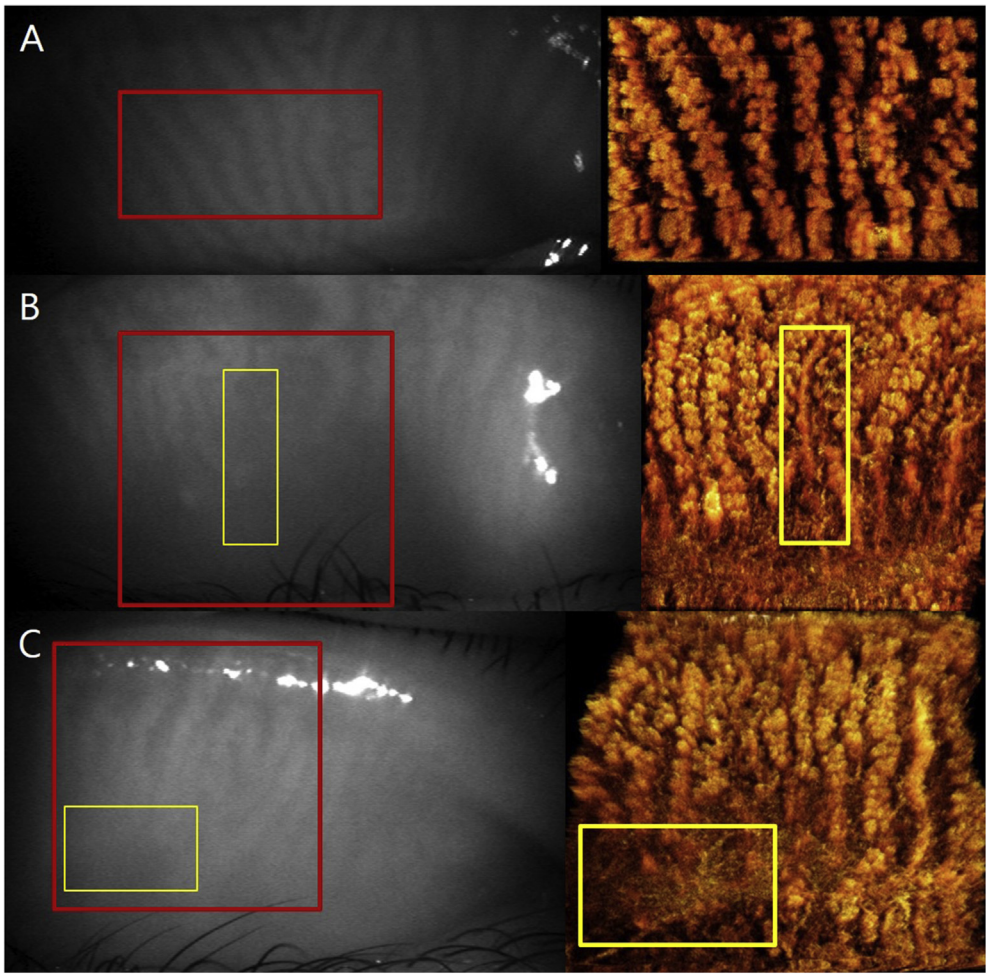


**Fig. 3.** Meibomian gland images from optical coherence tomography (OCT). Normal meibomian glands have uniform and properly sized acini (A). At the dropout lesion, the remaining duct is found in the deep layer (B). At the dropout lesion, we can observe a few acini in the deep layer (C). The area reconstructed using OCT is marked with a red rectangle (the measured area of A, B, and C were 4 × 2.8 mm, 4 × 4 mm, and 4 × 4 mm, respectively) and the dropout area on the infrared images is marked with a yellow rectangle.

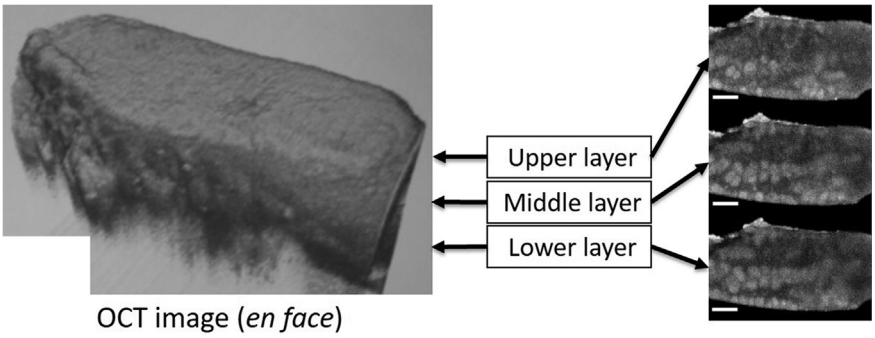


**Fig. 4.** Three imaging planes were selected from two-dimensional (2D) images at different levels. Depth information from optical coherence tomography imaging demonstrates this analysis. Left panel is a perspective view of a 3D rendered image and right panels are en face images. The white scale bar represents 1 mm.

segmentation of the acini from OCT images was used as a diagnostic tool for morphological evaluation. The lateral resolution and field-of-view of the real-time swept-source OCT system we used were 8.6 μm and 4.3 × 4.3 mm, respectively. In addition, we are now developing 3D software program for measuring the volume of acini in MGs. As a next step, we are preparing further quantification of entire volume of acini using a new developed 3D software program.

Recently, OCT technology was applied to histologic examination, which is called optical coherence microscopy (OCM). OCM can provide high-resolution transverse imaging by using high numerical aperture lenses because OCM does not depend on high axial resolution for optical sectioning (Leitgeb, 2017). OCM has an advantage of a large field-of-view and multi-scale imaging compared with confocal imaging. Anatomic structures in brain tissue could be differentiated on OCM images and this technique was comparable to traditional histology staining (Min et al., 2015).

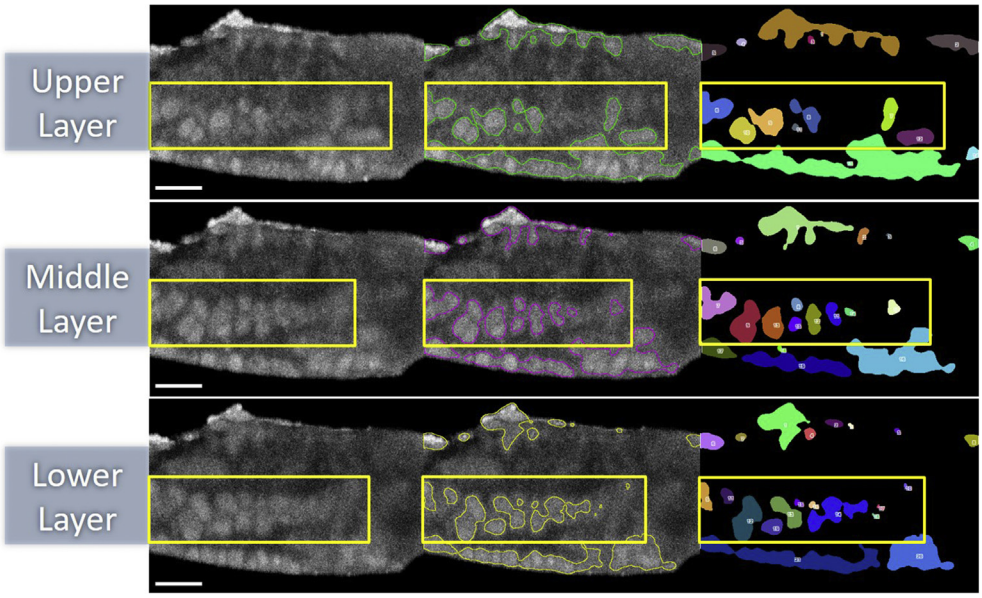


**Fig. 5.** Segmentation and calculation of the acinar area in the meibomian glands. A segmentation method is used in the quantification of the acini. Each acinus shows high contrast compared with other lesions. These contrast differences make segmentation of the acini possible. Each acinar area is filled with a different color in each image. The imaging plane of the upper layer is 0.8 mm below the palpebral conjunctiva. The middle and lower layers are 0.9 mm and 1.0 mm below the surface, respectively. The area analyzed using the segmentation method is marked with a yellow rectangle. The white scale bar represents 1 mm.

The application of OCM analysis to the study of meibomian glands would be another way to understand the pathophysiology in terms of structural changes of the acini and ducts in the meibomian glands.

## 6. Future of meibomian gland dysfunction diagnosis

Dry eye related to MGD was not explained by one parameter alone because of the pathophysiology of MGD. Although the pathophysiology has not been clearly revealed, MGD and dry eye share a vicious cycle and are interrelated (Geerling et al., 2017; Maskin and Thomas, 2007; Nichols et al., 2011; Tomlinson et al., 2011). The lipid component in the tear film and acini in the meibomian glands could be evaluated simultaneously in the diagnosis of MGD. Hence, quantitative analysis tools for acinar lipids should also be developed in the future so that lipid analysis of the tear film can be used in clinical settings. With these devices, a new fine-scale grading system also contributes to the diagnosis of MGD (Pult and Nichols, 2012; Nelson et al., 2011; Ngo et al., 2014).

## Funding

This work was supported by Basic Science Research Program through the National Research Foundation of Korea (NRF) funded by the Ministry of Education (2016R1A6A1A03010528).

## Conflict of interest

No conflicting relationship exists for any author.

## References

Arita, R., Itoh, K., Inoue, K., Amano, S., 2008. Noncontact infrared meibography to document age-related changes of the meibomian glands in a normal population. Ophthalmology 115, 911–915.
Arita, R., Itoh, K., Inoue, K., Kuchiba, A., Yamaguchi, T., Amano, S., 2009a. Contact lens wear is associated with decrease of meibomian glands. Ophthalmology 116, 379–384.
Arita, R., Itoh, K., Maeda, S., Maeda, K., Furuta, A., Fukuoka, S., Tomidokoro, A., Amano, S., 2009b. Proposed diagnostic criteria for obstructive Meibomian gland dysfunction. Ophthalmology 116, 2058–2063.
Arita, R., Itoh, K., Maeda, S., Maeda, K., Tomidokoro, A., Amano, S., 2010. Efficacy of diagnostic criteria for the differential diagnosis between obstructive meibomian gland dysfunction and aqueous deficiency dry eye. Jpn. J. Ophthalmol. 54, 387–391.
Arita, R., Suehiro, J., Haraguchi, T., Shirakawa, R., Tokoro, H., Amano, S., 2014. Objective image analysis of the meibomian gland area, 98, 746–755.
Arita, R., Minoura, I., Morishige, N., Shirakawa, R., Fukuoka, S., Asai, K., Goto, T., Imanaka, T., Nakamura, M., 2016. Development of definitive and reliable grading scales for meibomian gland dysfunction. Am. J. Ophthalmol. 169, 125–137.
Bron, A.J., Tiffany, J.M., 2004. The contribution of meibomian disease to dry eye. Ocul. Surf. 2, 149–165.
Finis, D., Pischel, N., Schrader, S., Geerling, G., 2013. Evaluation of lipid layer thickness measurement of the tear film as a diagnostic tool for Meibomian gland dysfunction. Cornea 32, 1549–1553.
Geerling, G., Baudouin, C., Aragona, P., Rolando, M., Boboridis, K.G., Benítez-Del-Castillo, J.M., Akova, Y.A., Merayo-Lloves, J., Labetoulle, M., Steinhoff, M., Messmer, E.M., 2017. Emerging strategies for the diagnosis and treatment of meibomian gland dysfunction: proceedings of the OCEAN group meeting. Ocul. Surf. 15, 179–192.
Hwang, H.S., Shin, J.G., Lee, B.H., Eom, T.J., Joo, C.K., 2013. In vivo 3D meibography of the human eyelid using real time imaging Fourier-domain OCT. PLoS One 8, e67143.
Ibrahim, O.M., Matsumoto, Y., Dogru, M., Adan, E.S., Wakamatsu, T.H., Goto, T., Negishi, K., Tsubota, K., 2010. The efficacy, sensitivity, and specificity of in vivo laser confocal microscopy in the diagnosis of meibomian gland dysfunction. Ophthalmology 117, 665–672.
Ibrahim, O.M., Matsumoto, Y., Dogru, M., Adan, E.S., Wakamatsu, T.H., Shimazaki, J., Fujishima, H., Tsubota, K., 2012. In vivo confocal microscopy evaluation of meibomian gland dysfunction in atopic-keratoconjunctivitis patients. Ophthalmology 119, 1961–1968.
Jester, J.V., Rife, L., Nii, D., Luttrull, J.K., Wilson, L., Smith, R.E., 1982. In vivo biomicroscopy and photography of meibomian glands in a rabbit model of meibomian gland dysfunction. Invest. Ophthalmol. Vis. Sci. 22, 660–667.
Kent, C., 2013. Breaking new ground in meibography. Rev. Ophthalmol. Published 8 July.
Knop, E., Knop, N., Millar, T., Obata, H., Sullivan, D.A., 2011. The international workshop on meibomian gland dysfunction: report of the subcommittee on anatomy, physiology, and pathophysiology of the meibomian gland. Invest. Ophthalmol. Vis. Sci. 52, 1938–1978.
Leitgeb, R., Hitzenberger, C., Fercher, A., 2003. Performance of fourier domain vs. time domain optical coherence tomography. Opt. Express 11, 889–894.
Leitgeb, R.A., 2017. Optical coherence microscopy. Methods Mol. Biol. 1563, 167–182.
Lemp, M.A., Crews, L.A., Bron, A.J., Foulks, G.N., Sullivan, B.D., 2012. Distribution of aqueous-deficient and evaporative dry eye in a clinic-based patient cohort: a retrospective study. Cornea 31, 472–478.

Liang, Q., Pan, Z., Zhou, M., Zhang, Y., Wang, N., Li, B., Baudouin, C., Labbé, A., 2015. Evaluation of optical coherence tomography meibography in patients with obstructive meibomian gland dysfunction. Cornea 34, 1193–1199.
Maskin, S.L., Thomas, P., 2007. The Causes. Reversing Dry Eye Syndrome. Yale University Press, pp. 44–71.
Matsumoto, Y., Sato, E.A., Ibrahim, O.M., Dogru, M., Tsubota, K., 2008. The application of in vivo laser confocal microscopy to the diagnosis and evaluation of meibomian gland dysfunction. Mol. Vis. 14, 1263–1271.
Messmer, E.M., Torres Suarez, E., Mackert, M.I., Zapp, D.M., Kampik, A., 2005. In vivo confocal microscopy in blepharitis. Klin. Monatsbl. Augenheilkd. 222, 894–900.
Min, E., Lee, J., Vavilin, A., Jung, S., Shin, S., Kim, J., Jung, W., 2015. Opt. Lett. 40, 4420–4423.
Milner, M.S., Beckman, K.A., Luchs, J.I., Allen, Q.B., Awdeh, R.M., Berdahl, J., Boland, T.S., Buznego, C., Gira, J.P., Goldberg, D.F., Goldman, D., Goyal, R.K., Jackson, M.A., Katz, J., Kim, T., Majmudar, P.A., Malhotra, R.P., McDonald, M.B., Rajpal, R.K., Raviv, T., Rowen, S., Shamie, N., Solomon, J.D., Stonecipher, K., Tauber, S., Trattler, W., Walter, K.A., Waring 4th, G.O., Weinstock, R.J., Wiley, W.F., Yeu, E., 2017. Dysfunctional tear syndrome: dry eye disease and associated tear film disorders - new strategies for diagnosis and treatment. Curr. Opin. Ophthalmol. (Suppl. 1), 3–47.
Napoli, P.E., Coronella, F., Satta, G.M., Iovino, C., Sanna, R., Fossarello, M., 2016. A simple novel technique of infrared meibography by means of spectral-domain optical coherence tomography: a cross-sectional clinical study. PLoS One. 11, e0165558.
Nelson, J.D., Shimazaki, J., Benitez-del-Castillo, J.M., Craig, J.P., McCulley, J.P., Den, S., Foulks, G.N., 2011. The international workshop on meibomian gland dysfunction: report of the definition and classification subcommittee. Invest. Ophthalmol. Vis. Sci. 52, 1930–1937.
Ngo, W., Srinivasan, S., Schulze, M., Jones, L., 2014. Repeatability of grading meibomian gland dropout using two infrared systems. Optom. Vis. Sci. 91, 658–667.
Nichols, K.K., Foulks, G.N., Bron, A.J., Glasgow, B.J., Dogru, M., Tsubota, K., Lemp, M.A., Sullivan, D.A., 2011. The international workshop on meibomian gland dysfunction: executive summary. Invest. Ophthalmol. Vis. Sci. 52, 1922–1929.
Nicolaides, N., Kaitaranta, J.K., Rawdah, T.N., Macy, J.I., Boswell 3rd, F.M., Smith, R.E., 1981. Meibomian gland studies: comparison of steer and human lipids. Invest. Ophthalmol. Vis. Sci. 20, 522–536.
Pult, H., Nichols, J.J., 2012. A review of meibography. Optom. Vis. Sci. 89, E760–E769.
Qiao, J., Yan, X., 2013. Emerging treatment options for meibomian gland dysfunction. ClinOphthalmol 7, 1797–1803.
Randon, M., Liang, H., El Hamdaoui, M., Tahiri, R., Batellier, L., Denoyer, A., Labbé, A., Baudouin, C., 2015. In vivo confocal microscopy as a novel and reliable tool for the diagnosis of Demodex eyelid infestation. Br. J. Ophthalmol. 99, 336–341.
Robin, J.B., Jester, J.V., Nobe, J., Nicolaides, N., Smith, R.E., 1985. In vivo transillumination biomicroscopy and photography of meibomian gland dysfunction. A clinical study. Ophthalmology 92, 1423–1426.
Salomatina, E., Jiang, B., Novak, J., Yaroslavsky, A.N., 2006. Optical properties of normal and cancerous human skin in the visible and near-infrared spectral range. J. Biomed. Opt. 11, 064026.
Srinivasan, S., Menzies, K., Sorbara, L., Jones, L., 2012. Infrared imaging of meibomian gland structure using a novel keratograph. Optom. Vis. Sci. 89, 788–794.
Tapie, R., 1977. Biomicroscopic study of the glands of meibomius. Ann. Ocul. 210, 637–648.
Tomlinson, A., Bron, A.J., Korb, D.R., Amano, S., Paugh, J.R., Pearce, E.I., Yee, R., Yokoi, N., Arita, R., Dogru, M., 2011. The international workshop on meibomian gland dysfunction: report of the diagnosis subcommittee. Invest. Ophthalmol. Vis. Sci. 52, 2006–2049.
Tong, L., Chaurasia, S.S., Mehta, J.S., Beuerman, R.W., 2010. Screening for meibomian gland disease: its relation to dry eye subtypes and symptoms in a tertiary referral clinic in Singapore. Invest. Ophthalmol. Vis. Sci. 51, 3449–3454.
Tsubota, K., Yokoi, N., Shimazaki, J., Watanabe, H., Dogru, M., Yamada, M., Kinoshita, S., Kim, H.M., Tchah, H.W., Hyon, J.Y., Yoon, K.C., Seo, K.Y., Sun, X., Chen, W., Liang, L., Li, M., Liu, Z., Asia Dry Eye Society, 2017. New perspectives on dry eye definition and diagnosis: a consensus report by the Asia dry eye society. Ocul. Surf. 15, 65–76.
Tuchin, V.V., 2007. Tissue Optics: Light Scattering Methods and Instruments for Medical Diagnosis, second ed. SPIE Press, Bellingham, WA, pp. 169–170.
Villani, E., Beretta, S., De Capitani, M., Galimberti, D., Viola, F., Ratiglia, R., 2011. In vivo confocal microscopy of meibomian glands in Sjogren's syndrome. Invest. Ophthalmol. Vis. Sci. 52, 933–939.
Yokoi, N., Komuro, A., Yamada, H., Maruyama, K., Kinoshita, S., 2007. A newly developed video-meibography system featuring a newly designed probe. Jpn. J. Ophthalmol. 51, 53–56.
Yoo, Y.S., Na, K.S., Byun, Y.S., Shin, J.G., Lee, B.H., Yoon, G., Eom, T.J., Joo, C.K., 2017. Examination of gland dropout detected on infrared meibography by using optical coherence tomography meibography. Ocul. Surf. 15, 130–138.